Hospital acquired infections: Biofilm assembly and increased antibiotic resistance of microorganisms

Maria Miguel Fachadas Bandeira
Instituto Superior Técnico, Universidade Técnica de Lisboa, Lisboa, Portugal.

***Abstract* — Healthcare-associated infections (HAIs) are a public health threat. The etiological agents responsible for these infections are diverse and often resistant to antibiotics. Bacteria are able to assemble biofilms persisting in healthcare units, becoming more resistant to antibiotic and being responsible for HAIs onset and spread.**

Bacteria isolated from samples, collected in hospitals fulfilling the criteria of HAI, were used. The selected bacteria comprise classical (*Klebsiella pneumoniae*) and emergent agents of HAI (Nontuberculous mycobacteria: NTM). Bacterial ability to assemble biofilms on cell culture plates was evaluated by the microtiter plate test. The structural features of bacteria (planktonic and biofilms) were accessed using scanning electron microscopy (SEM). Biofilms assembled on the model surface (cell culture plate) and on abiotic surfaces present in healthcare units (*e.g.* silicon) were characterized. For *K. pneumoniae* strains the ability to assemble biofilms on biotic surfaces (HeLa cells) was also evaluated.

The SEM analysis allowed the identification of differences between planktonic and sessile bacteria, which were linked to increased virulence. The results showed that biofilm assembly depends on bacteria and abiotic surface. On biotic surfaces, the biofilm assembly is dependent on tropism relations between bacteria and the host. For NTM biofilm was possible to identify factors involved in biofilm assembly: sliding and membrane charges. In the case of *K.pneumoniae* this relation was not establish. Nevertheless, it was possible to establish a link between the ability to assemble biofilm and increased antibiotic resistance. Altogether these data revealed a relation between biofilm assembly, antibiotic resistance and spread of HAIs.

Keywords
Antibiotic resistance, bacteria, biofilm assembly, healthcare-associated infection, SEM

I. INTRODUCTION

Healthcare-associated infections (HAIs) are a significant consequence of hospitalization. These infections are one of the leading causes of death and morbidity among hospitalized patients, occurring after 48h of hospitalization [1, 2, 3].

Factors such environmental or patient-related can contribute to the development of HAIs [4], however etiological agents are responsible for HAIs spread. These agents are bacteria, viruses, fungi and parasites [5, 6], being bacteria the most frequent one. Bacteria divide into Gram-negative and Gram-positive bacteria, according to cell wall composition. Gram-negative bacteria are hydrophilic [7, 8, 9] while Gram-positive are hydrophobic [7, 9, 10, 11]. In this study, both bacteria types are studied. Gram-negative bacteria considered in this study are *Klebsiella pneumoniae*, and Gram-positive bacteria belong to a group known as nontuberculous mycobacteria (NTM). *Klebsiella pneumoniae* is a classical agent of HAIs, being considered multirresistant bacteria [12]. Nontuberculous mycobacteria are recently known as a pathogenic agent, and have being increased their resistance to antibiotic action. Together with their cell wall composition, growing time is other difference between studied strains. Nontuberculous mycobacteria are considered rapid-growers among mycobacteria, however their generation time is much longer than *K.pneumoniae.*

Bacteria increase their resistance, organizing themselves in a biofilm, being 80% of infections caused by bacteria within biofilm [13]. Biofilms are described as colonies of microorganisms that are attached to each other and to a surface, in an irreversible mode [14, 15]. Biofilm assembly proceeds through the following phases: reversible attachment, irreversible attachment, maturation and dispersion [14, 16]. During attachment, planktonic bacteria adhere to surface through the sum of attractive and repulsive forces [14]. Bacterial *pili* also play a key role in attachment [17, 18]. Bacteria start to excrete the extracellular polymeric substance (EPS) that promote attachment [14, 19]. In maturation, the rate of replication of microorganisms increases until a mature biofilm is formed [14]. After maturation, bacteria suffer dispersion originating new biofilms in other surface areas [14, 19]. Biofilm assembly can be described as a cycling event (Figure 1).

As already mentioned, biofilms are the major cause of HAIs onset and spread. Among these infections are urinary tract infections, nosocomial pneumonia, bloodstream infection and endocarditis, all related to biofilm colonization on medical devices [20].

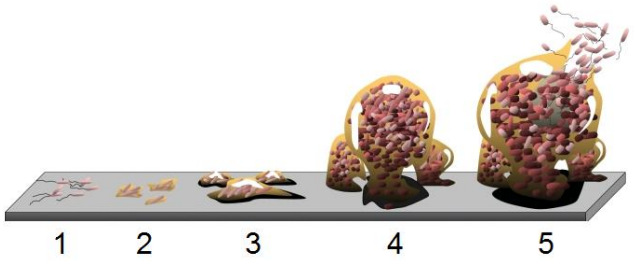

Figure 1 - **Temporal evolution of biofilm.**
The different phases of biofilm assembly: (1) reversible attachment, (2) irreversible attachment, (3,4) mature biofilm assembly and (5) dispersion are represented.
Adapted from Monroe, 2007 [16].

Healthcare-associated infections can be difficult to treat due to bacterial resistance to antibiotics [21]. Bacteria within biofilm become more resistant, surviving to adverse conditions. Antibiotic may fail to penetrate through biofilm, due to extracellular matrix, that limit the transport of antimicrobial agents [22, 23]. However, studies have shown that biofilm matrix is not the only reason of bacterial resistance [24]. Bacteria within biofilm have created mechanisms for antimicrobial action. Mutations, resulting on horizontal gene transmission can modify antibiotic targets, promote efflux pumps and enzymes production [9, 20, 25, 26, 27]. Enzymatic inhibition inactivates various antibiotics, recognizing them and changing their functional characteristics [9, 26]. Efflux pumps allow antibiotic excretion from the cell membrane [9, 26]. Molecules have been synthesized to inhibit cell-to-cell communications (quorum-sensing - QS). Those molecules are denominated by quorum-sensing inhibitors (QSIs). This cell-to-cell communication can regulate the production of virulence factors, protecting bacteria against phagocytes and influencing the development of the biofilm [20]. Also, mature biofilms have developed different resistance mechanisms. The antibiotic can be deactivated in the first layers of biofilm. Altering biofilm microenvironment (*e.g.* oxygen and pH levels), leads to slow growth of bacteria, reducing their susceptibility [20]. Other defense mechanism is the phenotypic states changing, promoting variations in colony morphology, enhancing virulence and antimicrobial resistance [28, 29, 30].

To avoid increase resistance of bacteria, there should be a prudent use of antibiotics avoiding overuse and inappropriate use.

II. Materials and Methods

a. Biological Samples

Three reference bacteria strains and four clinical strains were evaluated in this study. Reference strains are *M. smegmatis* mc^2155, *M. fortuitum* ATCC 6841 and *M. chelonae* ATCC 35752. Clinical strains are *M. fortuitum* 747/08, isolated from sputum, *K. pneumoniae* 2948 and *K. pneumoniae* 703;O:1, both isolated from urine and *K. pneumoniae* 45 isolated from colonization studies (neck swab). All strains were grown either using Mueller-Hinton broth or Mueller-Hinton agar. *Klebsiella pneumoniae* were incubated overnight and mycobacteria were incubated for 72h at 37ºC.

HeLa cells were used for study bacterial adhesion to a biotic surface. Cells were culture in DMEM (Lonza) supplemented with 10% heat inactivated fetal calf serum (Difco), 1% glutamine (Difco), 1% non essential aminoacids (Difco), 10,000 IU of penicillin (Difco), 10µg streptomycin (Difco) and incubated for 2days at 37ºC with 5% CO_2.

b. Bacteria susceptibility to antibiotics

The antimicrobial activity of amoxicillin (BioRad), fosfomycin (BioRad), gentamicin (Gibco) and vancomycin (BioRad) was evaluated by the microdilution method. Briefly, antibiotics were diluted in Mueller-Hinton broth to produce a two-fold dilution in the concentrations range of 10000 – 0.0048µg/mL for amoxicillin, 500 – 0.244 µg/mL for fosfomycin, 12500 – 0.191µg/mL for gentamicin and 1000 – 0.244 µg/mL for vancomycin. A positive control containing a suspension of bacteria in Mueller-Hinton broth without antibiotics was performed in parallel. The MIC was defined as the lowest concentration of antibiotic resulting in the absence of turbidity after over-night incubation at 37ºC.

The minimum inhibitory concentration for biofilm was performed using the same antibiotics and concentrations range. After removing the non-adherent bacteria the antibiotic solutions were added, the attached bacteria were sonicated in a water table sonicator for 5 minutes and incubated over-night at 37ºC.

c. Bacteria generation time

All bacteria were grown in Mueller-Hinton broth being harvested after different incubation times. *Klebsiella pneumoniae* strains were harvested after 2, 4, 6, 10, 24 and 48 hours. Nontuberculous mycobacteria were harvested after 4, 8, 24, 48, 72 and 120hours. At each harvesting time bacterial optical density (OD) at 600 nm was determined in a spectrophotometer (SpectraMax 340PC). The obtained OD values were converted into bacteria concentration and the generation time for each bacterium was calculated.

d. Quantification of biofilm formation

The assay was performed in triplicate using 96-well flat-bottomed cell culture plates (Nunc) as described previously with small modifications [31]. Briefly, microorganism suspensions with a final concentration of 10^7 bacteria per milliliter were prepared in 0.9% sodium chloride and tenfold diluted in Mueller-Hinton broth (Difco). Two-hundred microliters of the bacterial suspension were distributed by each well being Mueller-Hinton broth used as negative control. The plates were incubated at 37ºC to allow biofilm formation for different time periods. Then, the content of each well was aspirated, and each well was vigorously washed three times with sterile distilled water to remove non-adherent bacteria. The attached bacteria were then stained for 15 minutes with 100 µl violet crystal at room

temperature, washed with distilled water three times to remove dye in excess and allowed to dry at room temperature. The violet crystal was dissolved in 100 µl of 95% ethanol (Merck) and the optical density at 570nm was read using a (SpectraMax 340PC).

e. Biofilm assembly on abiotic surfaces

Bacteria were allowed to assemble biofilm for different time periods on different surfaces. In all cases the incubation was performed at 37ºC in Mueller-Hinton broth.

Biofilm forming ability on abiotic surfaces was evaluated by microtiter-plate test [32]. Assembly was firstly performed on a chosen model, a 6-well flat-bottomed sterile cell culture plate (Nunc), and then on surfaces that mimic those present in healthcare units (silicon and stainless steel).

The assembly was performed according to bacteria growth. For *K. pneumonia*e chosen times were 4, 12, and 24 hours and for NTM were 1, 3 and 5 days. The assembly on stainless steel was only performed for *K. pneumoniae* for 12 hours.

f. Adherence assay on biotic surface

Adhesion assay was performed in a 24-well culture plate, being seeded 10^4 cells per well, prior to *K. pneumoniae* infection.

Bacteria were prepared from frozen stocks, incubating them for 18hours at 37ºC. Then bacteria were diluted (1:100) and incubated at 37ºC for 24hours. Cultures density was determined by OD measurement, at 600nm (SpectraMax 340 PC) and viable bacteria were quantified by CFU – colony forming unit.

Layers of HeLa cells were rinsed twice with 1mL of DMEM. Bacteria were harvested and rinsed twice with PBS and resuspended in DMEM with 2% D-mannose (Difco) without antibiotics. Then 0.1mL of this suspension was added per well and bacteria were allowed to adhere at 37ºC and in 5% CO_2 atmosphere for 4, 8 or 24 hours. Wells without cells were prepared in the same manner to control bacterial adhesion to plastic.

After the specified incubation times the wells were rinsed three times with 1mL of PBS. Adherent bacteria were released by adding 0.2mL of 0.5% Triton X-100 (Sigma) for 5 to 10minutes. Saline solution was added to each sample which was further diluted and plated in LB media. Adherent bacteria were quantified by CFU enumeration. Bacterial adhesion to cells was determined by total CFU number minus CFU number of bacteria adherent to well without cells.

g. Zeta potential assay

Klebsiella pneumoniae and all NTM were evaluated in this assay. A homogenous suspension of each bacteria were prepared in 0.9% sodium chloride solution and centrifuged at 2000rmp for 10minutes (Megafuge 1.0 Heraeus Instruments). The supernatant was discarded and the bacterial pellets were fixed with 4% PFA for 15 minutes at room temperature. Bacteria were washed with PBS and harvested by centrifugation at 2000 rpm for 10 minutes. The pellets were resuspended in PBS being the OD_{600nm} determined. Bacterial suspensions were then further processed in order to obtain a final OD_{600nm} of 0.4.

Zeta potential assay was determined using water (H_2O) pH = 6.3. The experiment was performed with a Malvern Zetasizer instrument (Zetasizer Nano ZS ZEN 3600, MALVERN). Briefly, bacterial suspensions were inserted into a disposable capillary cell.

h. Sliding motility assay

Nontuberculous mycobacteria strains were grown in M63 salts medium supplemented with 1mM magnesium chloride, 0.2% glucose, 0.5% casamino acids, ferrous chloride (10µM) and a micronutrient solution. M63 medium was solidified with either 0.17% or 0.3% agar (Difco). Twenty-five millilitres of sterile medium (65ºC) was dispensed per plate. Plates were allowed to remain at room temperature overnight and then were inoculated from colonies by poking with toothpick. The plates were sealed with parafilm and incubated at 37ºC, for 3 days. Bacterial spreading was then evaluated.

i. Scanning electron microscopy analysis

Sample preparation

After biofilm assembly, samples were prepared for scanning electron microscopy visualization under both secondary or backscattered electron beam. At the end of each time point, samples were chemically fixed with 2.5% glutaraldehyde (EMS), 0.05% ruthenium red (Sigma) in 0.2M sodium cacodylate, pH 7.4 (Sigma). Samples were post-fixed with 1% osmium tetroxide (EMS).

After fixation samples were dehydrated using ethanol in an increasing concentration: 30% ethanol twice for 15 minutes each time (only for samples analyzed under secondary electron beam); 50% ethanol twice for 15 minutes each; 80% ethanol twice for 15 minutes each; 95% ethanol twice for 15 minutes each; 100% ethanol three times for 20 minutes each. For secondary electron observation, after dehydration, the samples were immediately transferred onto glass slides, allowed to dry at room temperature and coated with carbon (with ~ 20 nm of thickness) using a Sputter Coater QISOT ES Quorum Technologies. The samples were mounted in a sample holder with carbon tape and analyzed with secondary electron beam, under a scanning electron microscope JSM-7100F JEOL.

For backscattered electron (BS) analysis samples were further embedded in Epon812 epoxy resin (EMS), i.e, incubated in propylenoxide (Merck) twice for 15 minutes, propyleneoxide : epon resin (2:1) for 30 minutes, propyleneoxide : epon resin (1:1) for 30 minutes and left over night in 100% epon resin. Two additional incubations in 100% epon resin for 2 hours were performed before samples were allowed to polymerize at 65º for 3 days.

Once polymerized the blocks were trimmed and sectioned using an ultramicrotone (Leica). Thin sections

were transferred to coverslips coated with 0.5% (m/v) gelatin and 0.05% (m/v) chromium potassium sulfate dodecahydrate (Panreac) and allowed to dry at room temperature. The sections were contrasted with saturated uranyl acetate in water, for 30 minutes, followed by Reynolds lead citrate for 3 minutes. Then the coverslips were transferred to glass slides and samples were coated and mounted as described above for secondary electron beam samples. Samples were analyzed with backscattered electron beam under a scanning electron microscope JSM-7100F JEOL.

An alternative procedure was adopted for biofilms assembled on silicon disks. These samples instead of being sectioned as described above were prepared as metallographic samples, by grinding and polishing. Grinding was performed using a 600, 800, 1200 and 2400 grit SiC paper. Polishing was performed with diamond particles 6, 3 and 1 microns in diameter. Samples were cleaned with 70% ethanol and dried with hot air. Both grinding and polishing were performed on a polisher at 150 rpm.

Samples were coated with carbon (20nm) and mounted in a sample holder with carbon tape, and analyzed under backscattered electron beam under an electron microscope JSM-7100F JEOL.

Data analysis

Scanning electron microscopy micrographs were analyzed using *Image J* software. The bacteria length and width of planktonic and biofilm organized bacteria were evaluated (Figure 2). The areas of the different biofilms components were also evaluated as shown in figure 3. Briefly, biofilm total area, the area occupied by bacteria, extracellular matrix and channels were determined. The relative areas occupied by each component were further calculated.

j. Statistical test

Results of at least three independent experiments were expressed as the means +/- standard deviation (SD). For the analysis of backscattered electron SEM data at least one hundred bacteria present in non-consecutive sections were evaluated. Statistical significance was assessed by the Student t-test (two-tailed). A p value of < 0.05 (*) was considered to be statistically significant.

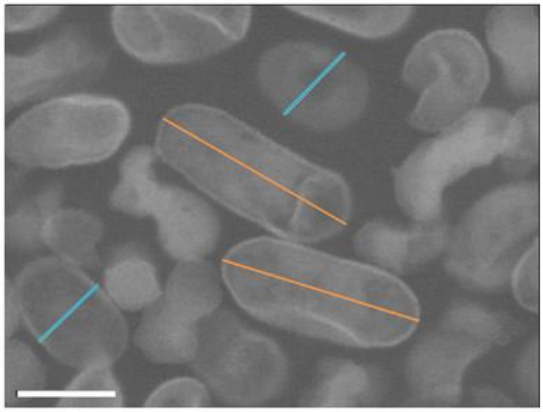

Figure 2 - **Bacterial dimensions determination.**
Bacterial dimensions were determined using Image J software. The length (orange line) and width (blue line) were determined measuring the strait lines drowned from the bacterial tips.
(Scale bar = 1µm)

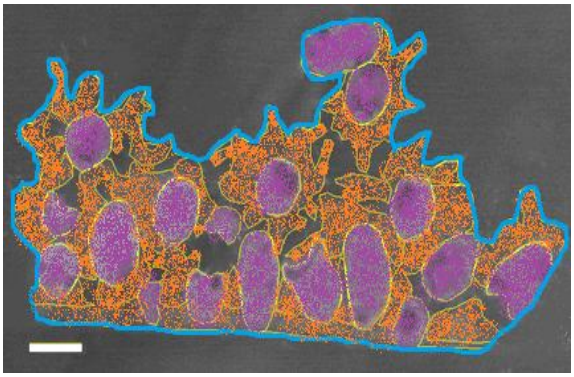

Figure 3 – **Biofilm constituints.**
Bacteria area (purple), extracellular matrix area (orange) and selected total biofilm area (blue) are represented.
(Scale bar = 1µm)

III. Results and Discussion

a. Gram-negative bacteria: *Klebsiella pneumoniae*

In this work three strains of *K. pneumoniae* were studied. Two of them are capsulated (*K. pneumoniae* 45 and *K. pneumoniae* 2948) and the other one is uncapsulated (*K. pneumoniae* 703;O:1). First structural features of bacteria were evaluated by SEM. Micrographs of planktonic bacteria were obtained by backscattered electron beam, and a significant number of bacteria were measured in length and width. It has been concluded that *K.pneumoniae* strains have similar lengths and widths, being in good agreement with literature [33].

Next the growth profile and generation time of bacteria were evaluated. Both *K. pneumoniae* 45 and *K. pneumoniae* 703;O:1 revealed similar growth curves, differing on

generation time, where *K. pneumoniae* 45 exhibited longer generation time across time points.

The antibiotic efficacy against bacteria was evaluated by the minimum inhibitory concentration – MIC. This assay was performed for both planktonic and biofilm organized bacteria since we wanted to evaluate the role played by biofilms on increased antibiotic resistance by *K. pneumoniae*. All antibiotics successfully inhibit bacterial growth, with bacteria organized in biofilm being generically more resistant [34]. The highest MIC within biofilm was registered for amoxicillin independently of the *K. pneumoniae* strain.

Next, the biofilm assembly was evaluated. Biofilm assembly was first evaluated on a model surface – cell culture plate. The three *K. pneumoniae* strains exhibited the ability to assemble biofilms although following different kinetics (Figure 4).

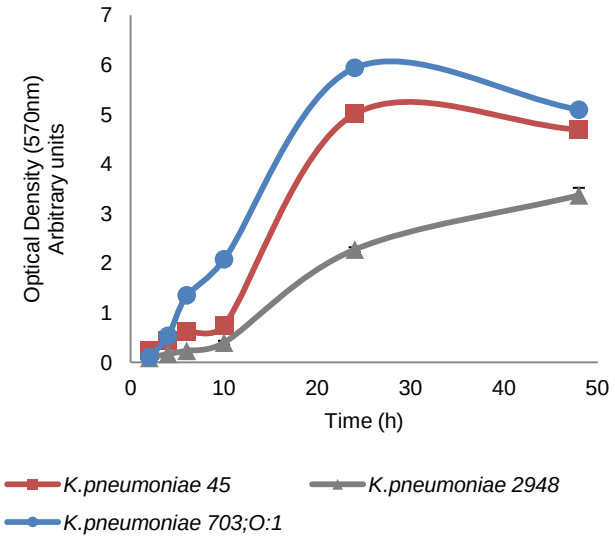

Figure 4 – **Kinetic of *K. pneumoniae* biofilm assembly.**

Two bacterial strains (*K. pneumoniae* 703;O:1 and *K. pneumoniae* 45) exhibited similar biomass growth profiles although the biomass increase was more significant for *K. pneumoniae* 703;O:1. The third bacterium (*K. pneumoniae* 2948) had the smallest amount of biomass. Based on these data, bacteria could be ranked concerning their biofilm assembly ability. The best biofilm assembler was *K. pneumoniae* 703;O:1 and the worse *K. pneumoniae* 2948, being *K. pneumoniae* 45 in an intermediate position.

It is important to establish a link between biofilm biomass evolution shown in figure 4 and biofilm phases described in the literature: attachment, maturation and dispersion [14]. Attachment stage is first identified, from 2 to 6 hours, where bacteria mass is starting to increase. Maturation ranges from 6 to 24 hours where biofilm reaches it maximum biomass. Last, dispersion starts at 24 hours and goes until 50 hours, where biomass is decreasing.

Once *K. pneumoniae* biofilm assembly kinetics was characterized we decided to evaluate their structure. For this purpose SEM techniques were used and allowed surface profiles observation. Through observation of obtained images, it was possible to confirm the biofilm assembly rank established before. *Klebsiella pneumoniae* 703;O:1 (Figure 5) was the best biofilm assembler, *K. pneumoniae* 2948 was the worse, while *K. pneumoniae* 45 was in intermediate position. We could also identify the phases of biofilm assembly mentioned previously. However, *K. pneumoniae* 45 revealed to have more difficult to surface attached, for reasons intrinsic to bacterium. *Klebsiella pneumoniae* 2948 exhibited maturation phase while the other two bacteria were already on dispersion phase. As discussed before, *K. pneumoniae* 2948 exhibited a different kinetic from the other two bacteria.

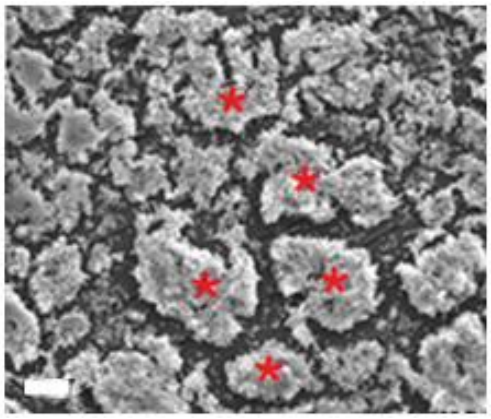

Figure 5 – **Biofilm of K. pneumoniae 703;O:1 assembled on cell culture plate.**
Mature biofilm is shown, being organized bacteria structures highlighted by red asterisks. (Scale bar=10µm)

The main differences between planktonic and biofilm organized form were identified. A comparison between images of planktonic and biofilm revealed the presence of extracellular matrix and a structural organization of bacteria within biofilm. Extracellular matrix (EPS) revealed to be important to maintain the structure of the biofilm, holding the biofilm together and protecting bacteria from stressful environmental conditions [35, 36]. Bacteria within biofilm are organized in a well-defined structure not randomly dispersed as in planktonic form. A schematic representation of a biofilm is shown in figure 6.

Figure 6 – **Schematic representation of a biofilm.**

In order to characterize the internal biofilm structure, we determined total biofilm area and then the areas occupied by

bacteria and extracellular matrix were measured [37]. Relative areas for bacteria and extracellular matrix within biofilm were calculated. The analysis of these data shows that the biofilms composition is different depending on the bacteria. *Klebsiella pneumoniae* 703;O:1 biofilms have higher amounts of bacteria whereas *K. pneumoniae* 45 biofilms are richer in extracellular matrix. In good agreement with the biofilm assay and the SEM micrographs revealing biofilm topography, *K. pneumoniae* 703;O:1 revealed to have the highest bacterial biomass at all biofilm assembly phases (Figure 7). At all time points, the relative area occupied by bacteria in *K. pneumoniae* 45 biofilms, was statistically smaller ($p<0.010$) than in both *K. pneumoniae* 703;O:1 and *K. pneumoniae* 2948 biofilms, showing that *K. pneumoniae* 45 biofilm is unique. Relative bacterial areas for the best (*K. pneumoniae* 703;O:1) and the worse (*K. pneumoniae* 2948) biofilm assembler only differ at later stages, being the relative area occupied by *K. pneumoniae* 703;O:1 bigger than by *K. pneumoniae* 2948 ($p<0.039$). These data shows that *K. pneumoniae* 703;O:1 and *K. pneumoniae* 2948 assembled similar biofilms although following different kinetics. As already mentioned, *K. pneumoniae* 45 biofilms consisted mostly in EPS, being this exacerbated production being explained by need of structures that promote bacterial attachment.

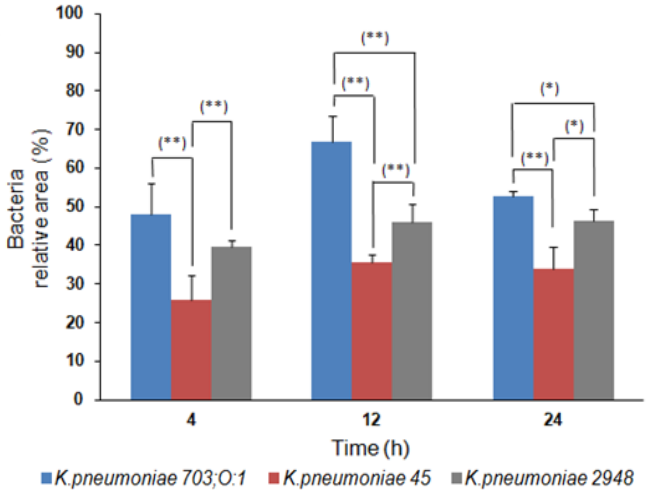

Figure 7 – **Characterization of *K. pneumoniae* biofilms assembled on cell culture plates.**
The relative amounts of bacteria were evaluated through biofilm evolution phases. (* $p<0.05$; ** $p<0.01$)

Once the ability to assemble biofilm on cell culture plate was confirmed, the next step was to test this ability on other surfaces. The chosen surfaces mimic those present in healthcare units, in order to study the contribution of biofilm assembly for HAIs spread. The selected materials were silicon and stainless steel. Silicon is used as coating of endoscopes and catheters, *e.g.* urinary catheters [38] and stainless steel is present in plumbing pipes in hospitals, and in water delivering-systems [39].

Silicon was the first evaluated surface. As described for cell culture plate, the phases of biofilm assembly could be identified and the biofilm assembly rank was kept unchanged. The differences observed in biofilm assembly for *K. pneumoniae* 45 and *K. pneumoniae* 2948 had also kept unchanged on silicon biofilms. Despite this fact, the biofilms assembled on silicon were denser than on cell culture plate, for all strains.

For stainless steel surface, this work was focused on only one time point (maturation) chosen with the assumption that biofilm assembly will follow a kinetic similar to the previously described. The biofilm assembly rank was kept unchanged, concordant to described for previous surfaces. In comparison with cell culture plate and silicon, the metallic surface revealed to be less suitable for biofilm assembly. It has been shown that hydrophobic, nonpolar surfaces (plastic) are more suitable for bacterial colonization than hydrophilic materials (metal) [40, 41].

After evaluating the biofilm assembly on abiotic surfaces, the adhesion to biotic surfaces *in vitro* was evaluated, to mimic *in vivo* interactions between bacteria and human cells. The adhesion assay was performed to evaluate the existence of preferential bacterial adhesion to a model of epithelial cells (HeLa cells). The existence of preferential adhesion to HeLa cells was translated by existence of colony forming units (Table 1).

Table 1 – **Adhesion assay.**

Time (h)	Bacteria (CFU)					
	K.pneumoniae 45		*K.pneumoniae* 703;O:1		*K.pneumoniae* 2948	
	Average	SD	Average	SD	Average	SD
4	4.25E+06	7.07E+04	-	-	-	-
8	6.60E+06	5.66E+04	-	-	-	-

The results shown that only *K. pneumoniae* 45 adheres preferentially to human cells, however HeLa cells are not able to phagocyte this bacterium. This preferential adhesion can be due to cell tropism [42]. As referred before, *K pneumoniae* 45 was isolated from skin (neck scrub). The cells present in this sample and HeLa cells are both epithelial which could explain the tropism of *K pneumoniae* 45. In opposition, *K. pneumoniae* 703;O:1 which did not show preferential adhesion to HeLa cells, was phagocytized being observed within the cytoplasm [Figure 8).

Figure 8 – **Phagocytized *K. pneumoniae* 703;O:1.**
Optical microscopy micrograph shown *K. pneumoniae* 703;O:1 being part of cell cytoplasm. Bacteria phagocytized are highlighted by red circles.

The selective phagocytosis of *K. pneumoniae* 703;O:1 could be explained by the absence of a capsule. This bacterium was the only studied bacterium devoid of capsule. The presence of a capsule is related to virulence, protecting bacteria from ingestion by phagocytes [43]. Other identified structures contributing to microorganism's enhanced virulence were *pili* and EPS. *Pili* are related to initial bacterial attachment, promoting adherence to host and contributing to increased virulence of pathogens [44]. Excreted EPS increases bacterial virulence by preventing antibiotics to reach their bacterial targets.

Altogether our data show that biofilm assembly in abiotic and biotic surfaces follows different rules. Despite this fact, several players collectively referred as virulence factors, are involved in the final outcome.

b. Gram-positive bacteria: Nontuberculous mycobacteria

Nontuberculous mycobacteria (NTM) are heterogeneous group of microorganisms including environmental bacteria and human pathogens. In this work, four NTM strains were used: *Mycobacterium smegmatis* mc^2155, *M. fortuitum* 747/08, *M. fortuitum* ATCC 6841 and *M. chelonae* ATCC 35752. Nontuberculous mycobacteria antibiotic susceptibility is determined by the minimum inhibitory concentration as described before for *K. pneumoniae* [45]. Most of strains are resistant to antibiotics, revealing an increase of MIC value in biofilm organized form [46].

The NTM strains were studied following the same strategy described for *K. pneumoniae*. Micrographs of planktonic bacteria were obtained by SEM, under backscattered electron beam, and a significant number of bacteria were measured in length and width. The obtained cell dimensions were in good agreement with literature [47]. Nontuberculous mycobacteria strains cells were similar in length and width, except for *M. fortuitum* ATCC 6841 which both length and width are different from other studied NTM strains.

Bacterial growth profile and generation time were evaluated. Nontuberculous mycobacteria behave differently from *K. pneumoniae* strains. These strains need longer incubation time to reach a significant number of bacteria. Although they have longer growth time in comparison to *K. pneumoniae* strains, they have a specific growth pattern. They are considered rapid-growers among mycobacteria genus. Regarding to evolution of generation time, NTM and *K. pneumoniae* strains behave in a similar way. As the incubation time increases, the generation time of bacteria decreases, resulting in faster bacterial division. Nontuberculous mycobacteria divide slower than *K. pneumoniae* being generation time at 24h 6-times slower for NTM than for *K. pneumoniae* strains.

Next the biofilm assembly ability was tested. Biofilm assembly was first evaluated on a model surface (cell culture plate). For NTM biofilm assembly was assessed for different periods of time due to its longer generation times, comparing to *K. pneumoniae.* Kinetic of biofilm assembly, for NTM, is shown in figure 9.

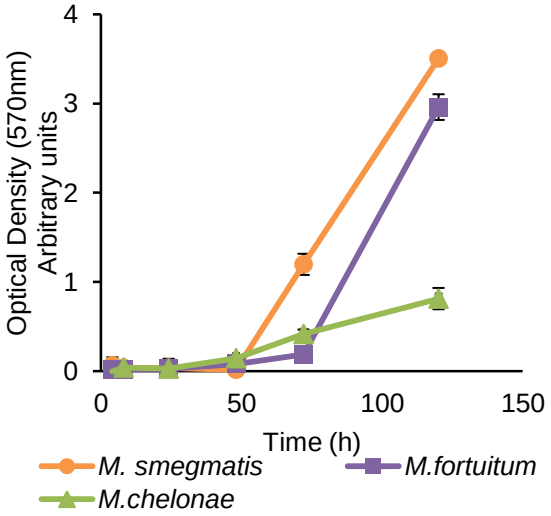

Figure 9 – **Kinetic of NTM biofilm assembly.**

Initially all strains followed a similar kinetic, while they are adapting to surface conditions. *Mycobacterium chelonae* was the bacterium that assembled less biofilm in initial stage, due to its longer generation time at early hours, exhibiting a different kinetic comparing to other strains. Bacterial growth biomass profiles were similar for both *M. smegmatis* and *M. fortuitum*, although *M. smegmatis* biomass increase was more pronounced. For NTM we followed only the two initial phases of biofilm assembly: attachment and maturation. The long generation time of these bacteria raised several experimental constraints, which do not allow following the biofilm development until dispersion. Despite this fact, biofilm assembly ability rank can be established: both *M. smegmatis* and *M. fortuium* were very similar in biofilm assembly ability, while *M. chelonae* revealed to be the worse biofilm assembler.

The internal structure of biofilms was also characterized, as proceeded for *K. pneumoniae*. *Mycobacterium smegmatis* biofilm had higher amounts of bacteria while *M. chelonae* biofilm had more extracellular matrix in its composition. These data are in good agreement with the biofilm assay. Mature biofilms of both *M. smegmatis* and *M. fortuitum* exhibited similar amounts of biomass (Figure 10). The relative area occupied by *M. chelonae* in mature biofilms was smaller than in the other NTM biofilms. The difference was significant when compared to *M. fortuitum* ($p=0.006$). As referred before, *M. chelonae* biofilm assembly ability was lower than for the other two strains, due to its biofillm assembly kinetic. The area occupied by extracellular matrix was higher for *M. chelonae*. As already discussed, the EPS production will increase to help bacteria attach to a surface, and *M. chelonae* revealed to be the NTM less prone to assemble biofilm. Altogether it can be claimed that, in spite the distinct kinetics *K. pneumoniae* and NTM are governed by the same factors.

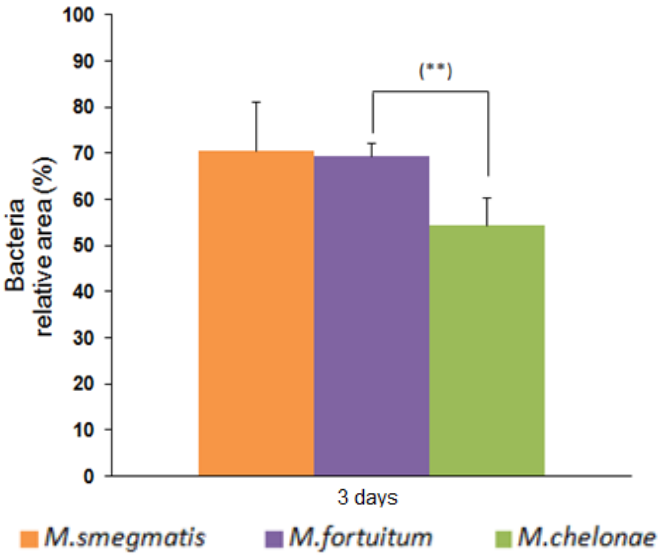

Figure 10 – **Characterization of NTM biofilms assembled on cell culture plates.**
The relative amounts of bacteria were evaluated. (** $p<0.01$)

Nontuberculous mycobacteria revealed a particular feature when comparing to *K. pneumoniae*. Biofilms on cell culture plates were assembled on two distinct interfaces. The bottom of the cell culture plate (solid-liquid interface) and the liquid surface (air-liquid interface) as schematically illustrated in figure 11. However, this fact has already described by others, being this "new" biofilm similar to a pellicle [48, 49]. Through evaluation of air-liquid interface biofilm structure, it was possible to conclude that floating biofilms were denser and more compact than bottom biofilms. This thickness can be explained by the fact that on air-liquid interface bacteria are in contact with both gaseous and liquid phases, having privileged access to all nutrients of both phases, *e.g.*, oxygen [50].

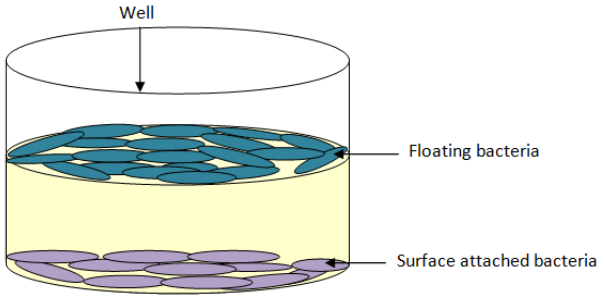

Figure 11 – **Outline of air-liquid assembly, for one NTM strain.**
Bacteria not only attached on cell culture bottom surface (purple) but also formed a pellicle covering the liquid surface (blue).

To give support to previous conclusion, biofilms assembled by the same bacterium on different interfaces and with different ages, were compared. The results shown that 1 day old floating biofilm was denser than 3 days old bottom biofilm. At higher magnifications, it was possible to observe the differences in bacteria structure. Bacteria within air-liquid biofilms were "fused" with each other whereas in the other interface they were individualized. The fusion phenomenon is mainly due to the presence of higher amounts of EPS.

The internal structure of floating biofilms was also evaluated, revealing an increase of bacteria mass for all strains. This means that NTM had more ability to assembly biofilm on air-liquid interface, for the reasons already described. Altogether our data showed that NTM are prone to form air-liquid biofilms in good agreement with the fact of being aerobic microorganisms and highly hydrophobic. This fact could account for the high rate of NTM found in water distribution systems.

Last, the biofilm assembly was evaluated on silicon. These biofilms obeyed to the biofilm assembly phases described in literature, increasing bacteria number between attachment and maturation phases. All bacteria exhibited less biomass on silicon surface than on other studied surfaces. This means that NTM strains had less ability to assemble biofilm on silicon. Nevertheless, the rank for biofilm assembly within NTM tested was kept unchanged.

The fact that NTM strains were less prone to assemble biofilm on silicon can be explained by surface and membrane charges. The fact that both silicon and NTM are hydrophobic could account for this outcome. During attachment superficial charges play a key role [51]. If bacteria and the attachment surface have the same charge the attachment will be hampered since a repulsive phenomenon will be generated.

c. Exploring factors involved on biofilm assembly

The last part of this work was an attempt to understand the factors involved in biofilm assembly. Among this we evaluated zeta potential, electrophoretic mobility and bacteria ability to move independently of flagella (sliding).

Zeta potential and electrophoretic mobility (EM) values are related to bacterial membrane charges and biofilm assembly [52]. As these values decrease, biofilm forming ability also decreases [53], and bacterial strains with heterogeneity in zeta potential and EM adhere better to surface, being more capable of assemble biofilm. All tested bacteria were negatively charged, and zeta potential and EM values followed the same tendency. For NTM, data were in good agreement with the literature. *Mycobacterium fortuitum* exhibited a lower zeta potential value than *M. smegmatis*, but it was more heterogeneous [52]. This fact could explain the alternation between both mycobacteria in biofilm assembly in different experimental conditions. *Mycobacterium chelonae*, the bacterium less prone to assemble biofilm, exhibited the lowest zeta potential as expected. The same conclusion was not possible to achieve for *K. pneumoniae*, probably due to differences in both bacterial strains cell wall.

Sliding mechanisms were also evaluated, being related to biofilm assembly ability [15]. Nontuberculous mycobacteria sliding ability was evaluated on both M63 medium with 0.3% and 0.17% agar. On the first medium (semi-solid medium) bacteria allowed to grow on the surface from the inoculation point, surrounding it with a circular halo. This halo diameter size is correlated with the ability of bacteria to pack cells within the monolayer [54]. *Mycobacterium smegmatis* (Figure 12.A) and *M. fortuitum* exhibited similar halos, which are bigger than the halo exhibited by *M. chelonae*. These data were in good agreement to established biofilm ability rank. *Mycobacterium chelonae* revealed to be a peculiar bacterium, having high content in porins within the cell wall [55, 56] being the less hydrophobic mycobacteria. This fact could account for its performance both on sliding and biofilm assembly assays.

On plates with lower agar concentration, bacteria growth exhibited a finger-like extension pattern initiated on the inoculation point, being notorious the ability of the best biofilm assemblers to spread (Figure 12.B).

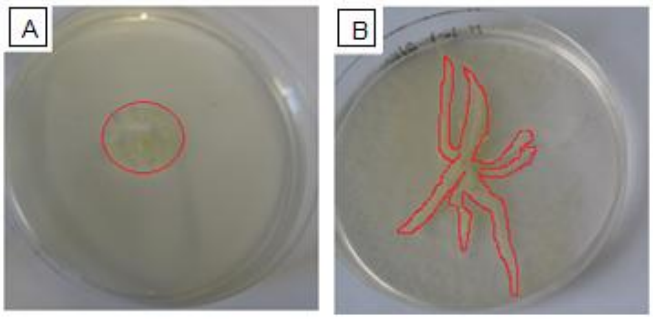

Figure 12 – **Evaluation of NTM sliding mobility.**
Spreading of NTM was evaluated. First strains were allowed to grow in semi-solid medium with *M. smegmatis* (A) and exhibiting larger halo (red circle). To exacerbate bacteria sliding a medium with 0.17% agar was used. *Mycobacterium. smegmatis* (B) growth exhibited finger-like extensions from the initial inoculation point (enhanced by red contouring).

IV. CONCLUSIONS

All bacteria tested had the ability to assemble biofilms. Nevertheless, biofilm assembly followed different kinetics and bacteria exhibited propensity for the different surfaces evaluated. In general, *K. pneumoniae* strains had more ability to assemble biofilm on silicon. This explains the high rates of colonization in catheters and endoscopes. Nontuberculous mycobacteria had more ability to assemble biofilm on air-liquid interface, being mostly common in water-distribution systems. *Klebsiella pneumoniae* 703;O:1 was the bacterium with the best performance among the Gram-negative bacteria. Two of the three NTM tested *M.smegmatis* and *M.fortuitum*, revealed similar ability to assemble biofilms.

Biofilm assembly was also performed on biotic surfaces. Here biofilm assembly was governed by factors distinct from abiotic surfaces. The bacteria tropism for host cells is an important factor. Additionally, bacteria features such as presence / absence of capsule were crucial for bacteria fate.

Bacterial generation time had influence on biofilm assembly, being crucial for bacteria organization within biofilm. Other factors as membrane charges and sliding properties play a key role on biofilm assembly ability. For NTM a link between these factors and biofilm assembly was established. However, for *K. pneumoniae* this relation could not be achieved. A more detailed study exploring bacteria properties such as cell wall composition could bring more insights in this issue.

All studied bacteria were susceptible to tested antibiotics *in vitro*. However, bacteria within biofilm could enhance their resistance to antibiotics up to 1000-fold as compared with the ones in planktonic form. Several virulence factors, crucial for increased resistance of microorganisms, have been identified. Factors within biofilm or intrinsic to bacteria revealed influence on bacteria increased resistance to antibiotics. These data revealed that a link between biofilm assembly, antibiotic resistance and spread of HAIs can be established.

V. FUTURE WORK

Bacterial adhesion to biotic surfaces revealed evidence of tropism and of being ruled by factors distinct from abiotic surfaces. More detailed studies in this area should be conducted to confirm the tropism, *e.g.*, using bladder epithelium cells for *K. pneumoniae*. The identification of the factors and the mechanisms involved in biofilm assembly in vivo are an important topic of study that should be carried out.

The study of a biofilm, assembled on a certain surface, as a living entity using RNA sequencing could improve our knowledge. This experimental approach might allow the identification of specific targets on different stages of biofilm assembly. If this targets are drugable new strategies either to avoid or eradicate biofilms could be developed. Among the strategies to avoid biofilm assembly would be the development of surface that inhibits bacterial growth. Coatings that function as inhibitors could also be a solution, for preventing biofilm assembly on medical devices.

REFERENCES

[1] Calfee, D. P. 2012. Crisis in hospital-Acquired healthcare-associated infections. Annual Review of Medicine. Vol. 63: 359-371.L

[2] Musau, J. 2013. The impact of healthcare-associated infections disease outbreaks on the nature of the healthcare professionals daily work. McMaster University.
[3] Shetty, N. 2009. Infectious diseases: Pathogenesis, prevention and case studies - Chapter 14. Wiley-Blackwell
[4] Devrajani, B. R., Shah, S. Z., Devrajani, T. and Qureshi, G. A. 2009. Nosocomial infections in medical ward (four months.
[5] Prevention of hospital-acquired infections – A Pratical Guide. 2nd Edition. World Health Organization. Department of Communicable Disease, Surveillance and Response.
[6] Aitken, C. and Donald, J. J. 2001. Nosocomial spread of viral disease, Clinical Microbiology Reviews. Vol. 14. No. 3. p. 528-546.
[7] Araújo, E. A., de Andrade, N. J., de Carvalho, A. F., Ramos, A. M., Silva, C. A., da Silva, L.H. M. 2010. Aspectos coloidais da adesão de micro-organismos. Quim. Nova. Vol. 33. No. 9. 1940-1948.

[8] Takeuchi, O., Hoshino, K., Kawai, T., Sanjo, H., Takada, H., Ogawa, T., Takeda, K., Akira, S. 1999. Differential roles of TLR2 and TLR4 in recognition of Gram-negative and Gram-positive bacterial cell wall components, Immunity; 11(4):443-51.

[9] Taylor, P. 2011. Combating intrinsic antibiotic resistance in Gram-negative. Open Dissertations and Theses. McMaster University.

[10] Mamo, W. 1989. Physical and biochemical surface properties of Gram-positive bacteria in relation to adhesion to bovine mammary cells and tissues. Rev. sci. tech. Off. int. Epiz., 8 (1), 163-176.

[11] Recth, J. and Kolter, R. 2001. Glycopeptidolipd acetylation affects sliding motility and biofilm formation in *Mycobacterium smegmatis*. Journal of Bacteriology. 183(19):5718-24.

[12] Moreira, V. C. and Freire, D. , *Klebsiella pneumoniae* e sua resistência a antibióticos.

[13] Pang, J. M., Layre, E., Sweet, L., Sherrid, A., Moody, D. B., Ojha, A. and Sherman, D. R. 2011. The Polyketide Pks1 contributes to biofilm formation in *Mycobacterium tuberculosis*. J Bacteriol.;194(3):715-21.

[14] Trinidad, A., Ibáñez, A., Gómez, D., Carcía-Berrocal, J. R. and Ramiréz-Camacho, R. 2010. Application of environmental scanning electron microscopy for study of biofilms in medical devices. Microscopy: Science, Technology, Applications and Education. A. Méndez-Vilas and J. Díaz (Eds.).

[15] Shi, T., Fu, T., Xie, J. 2011. Polyphospate deficiency affects the sliding motility and biofilm formation of *Mycobacterium smegmatis*. Curr Microbiol.;63(5):470-6.

[16] onroe, D. 2007. Looking for chinks in the armor of bacterial biofilms. PLoS Biol. ;5(11):e307.

[17] Proft, T. and Baker, E. N. 2009. *Pili* in Gram-negative and Gram-positive bacteria – structure, assembly and their role in disease. Cell Mol Life Sci.;66(4):613-35.

[18] Davey, M. E. and O'Toole, G. A. 2000. Microbial Biofilms: from ecology to molecular genetics. Microbiology and molecular biology reviews. 847-867.

[19] Abed, S. E., Ibnsouda, S. K., Latrache, H. and Hamadi, F. 2012. Scanning Electron Microscopy (SEM) and environmental SEM: Suitable tools for study of adhesion stage and biofilm formation. Scanning Electron Microscopy.

[20] Hoiby, N., Bjarnsholt, T., Givskov, M., Molin, S. and Ciofu, O. 2010. Antibiotic resistance of bacterial biofilms, International Journal of Antimicrobial Agents 35. p.322-332.

[21] Herdman, R. R. 1995. Impacts of Antibiotic-Resistant Bacteria.

[22] Mah, E. F. and O'Toole, G. A. 2001. Mechanisms of biofilm resistance to antimicrobial agents. Trends Microbiol.;9(1):34-9.

[23] Teng, R. and Dick, T. 2003. Isoniazid resistance of exponentially growing *Mycobacterium smegmatis* biofilm culture. FEMS Microbiology Letters. Vol. 227. Issue 2. p. 171-174.

[24] Anderl, J.N., Franklin, M. J. and Stewart, P. S. 2000. Role of antibiotic penetration limitation in *Klebsiella pneumoniae* biofilm resistance to ampicillin and ciprofloxacin. Antimicrob. Agents Chemother. 44, 1818–1824.

[25] Chamlagain, B. S. 2010. Characterization of antibiotic-resistant psychrotrophic bacteria in raw milk. University of Helsinki.

[26] Helt, C. 2012. Occurrence, fate, and mobility of antibiotic resistant bacteria and antibiotic resistance genes among microbial communities exposed to alternative wastewater treatment systems. University of Waterloo. Canada.

[27] Ito, A., Taniuchi, A., May, T., Kawata, K. and Okabe, S. 2009. Increased antibiotic resistance of *Escherichia coli* in mature biofilms. Appl Environ Microbiol.;75(12):4093-100.

[28] Stewart, P. S. and Costerton, J. W. 2001. Antibiotic resistance of bacteria in biofilms, Lancet.;358(9276):135-8.
[29] Corona, F. and Martinez, J. L. 2013. Phenotypic Resistance to Antibiotics. Antibiotics. 2*(*2), 237-255.

[30] Sousa, A. M. and Machado, I. 2011. Phenotypic switching: an opportunity to bacteria thrive. Science against microbial pathogens: communicating current research and technological advances. A. Mendéz-Vilas (Ed.).

[31] Stepanovic S., Vukovic D., Dakic I., Savic B. and Svabic-Vlahovic M., 2000, A modified microtiter-plate test for quantification of staphylococcal biofilm formation. *J Microbiol Methods.*, 40 :175-9.
[32] Agarwal, R. K.,Singh, S. Bhilegaonkar, K. N and Singh, V. P. 2011. Optimization of microtitre plate assay for the testing of biofilm formation ability in different Salmonella serotypes. International Food Research Journal. Vol.8 Issue 4. p. 1493-1498.

[33] Singh, V. Keshab, T. and Chauhan, P. K. 2012. Effect of poly herbal formulation against *Klebsiella pneumoniae* causing pneumonia in children's. Asian Journal of Pharmaceutical and Clinical Research. Vol.5. Suppl 1.

[34] Olson, M. E. Ceri, H., Morck, D. W., Buret, A. G. and Read, R. R. 2002. Biofilm bacteria: formation and comparative susceptibility to antibiotics. Can J Vet Res.;66(2):86-92.

[35] Cortés, M. E., Bonilla, J. C. and Sinisterra, R. D. 2011. Biofilm formation, control and novel strategies for eradication. Science against microbial pathogens: communicating current research and technologies advances.

[36] Koczan, J. M., Lenneman, B. R., McGrath, M. J. and Sundin, G. W. 2011. Cell surface attachment structures contribute to biofilm formation and xylem colonization by *Erwinia amylovora*. Applied and Environmental Microbiology. p. 7031-7039.

[37] Hall-Stoodley, L., Keevil, C. W. and Lappin-Scott, H. M. 1998. *Mycobacterium fortuitum* and *Mycobacterium chelonae* biofilm formsation under high and low nutrient conditions. Journal of Applied Microbiology. Vol. 85 Issue S1. p. 60S-69S.

[38] Niveditha, S. et al, 2012. The Isolation and the biofilm assembly of urophatogens in the patients with catheter associated urinary tract infections (UTIs).

[39] Percival, S. L., Knapp, J. S., Edyvean, R. G. K. and Wales, D. S. 1998. Biofilms, mains water and stainless steel. Water research. Vol. 32. Issue 7. p. 2187-2201.

[40] Donlan, R. M. 2002. Biofilms: microbial life on surfaces. Emerg Infect Dis.;8(9):881-90.

[41] Bendinger, B., Rijnaarts, H. H. M., Altendorf, K. and Zehnder, A. J. B. 1993. Physicochemical cell surface and adhesive properties of coryneform bacteria related to the presence and chain length of mycolic acids. Appl Environ Microbiol.;59:3973-77.

[42] Roberts, J. A. 1996. Tropism in bacterial infections:urinary tract infections. J Urol.;156(5):1552-9.

[43] Favre-Bonte, S., Darfeuille-Michaud, A. and Forestier, C. 1995. Aggregative adherence of *Klebsiella pneumoniae* to humam intestine-407 cells. Infect Immun.;63(4):1318-28.

[44] Mandlik, A., Swierczynske, A., Das, A. and Ton-That, H. 2007. Pili in Gram-positive bacteria: assembly, involvement in colonization and biofilm development. Trends Microbiol.; 16(1): 33–40.

[45] Gayathri, R., Therese, K. L., Deepa, P., Mandai, S. and Madhavan, H. N. 2010. Antibiotic susceptibility pattern of rapidly growing mycobacteria. J Postgrad Med.;56(2):76-8.

[46] Greendyke, R. and Byrd, T. F. 2008. Differential antibiotic susceptibility of *Mycobacterium abscessus* variants in biofilms and macrophages compared to that of planktonic bacteria. Antimicrob Agents Chemother.;52(6):2019-26.

[47] Silva, C., Perdigao, J., Alverca, E., de Matos, A. P., Carvalho, P. A., Portugal, I. and Jordão, L. 2013. Exploring the Contribuition of Mycobacteria Characteristics in Their Interaction with Humam Macrophages. Microsc Microanal.;19(5):1159-69.

[48] Khoo, B. and Gulati, P. 2013. Developing and mature biofilms produced by *Mycobacterium smegmatis*. American Society for Microbiology.

[49] Ojha, A. and Hatfull, G. F. 2007. The role of iron in *Mycobacterium smegmatis* biofilm formation: the exochelin siderophores is essential in limiting iron conditions for biofilm formation but not for planktonic growth. Molecular microbiology; 66(2). p. 468-483.

[50] Scher, K., Romling, U. and Yaron, S. 2005. Effect of heat, acidification, and chlorination on *Salmonella enterica serovar typhimurium* cells in a biofilm formed at the air-liquid interface. Appl Environ Microbiol.;71(3):1163-8.

[51] Borges, M. T., Nascimento, A. G., Rocha, U. N. and Tótola, M. R. 2008. Nitrogen starvation affects bacterial adhesion to soil. Brazilian Journal of Microbiology;39: p. 457-463

[52] Tariq, M., Bruijs, C., Kok, J. and Krom, B. P. 2012. Link between culture zeta potential homogeneity and Ebp in *Enterococcus faecalis*. Appl Environ Microbiol.; 78(7): 2282–2288.

[53] Pang, C. M., Hong, P., Guo, H. and Liu, W. T. 2005. Biofilm formation characteristics of
bacterial isolates retrieved from a reverse osmosis membrane. Environ Sci Technol.;39(19):7541-50.

[54] Martinéz, A., Torello, S. and Kolter, R. 1999. Sliding motility in mycobacteria. J Bacteriol.; 181(23): 7331–7338.

[55] van Houdt, R., Aertsen, A., Jansen, A. Quintana, A. L. and Michiels, C. W. 2004. Biofilm formation and cell-to-cell signaling in Gram-negative bacteria isolated from a food processing environment. J Appl Microbiol.;96(1):177-84.

[56] Nikaido, H., Kim, S. and Rosenberg, E. Y. 1993. Physical organization of lipids in the cell wall